Aerosol Science and Technology

ISSN: 0278-6826 (Print) 1521-7388 (Online) Journal homepage: https://www.tandfonline.com/loi/uast20

Soot mass concentration sensor using quartz-enhanced photoacoustic spectroscopy

Philipp Breitegger, Mario A. Schriefl, Robert T. Nishida, Simone Hochgreb & Alexander Bergmann

To cite this article: Philipp Breitegger, Mario A. Schriefl, Robert T. Nishida, Simone Hochgreb & Alexander Bergmann (2019) Soot mass concentration sensor using quartz-enhanced photoacoustic spectroscopy, Aerosol Science and Technology, 53:9, 971-975, DOI: 10.1080/02786826.2019.1635677

To link to this article: https://doi.org/10.1080/02786826.2019.1635677

Published online: 16 Jul 2019.

AEROSOL SCIENCE AND TECHNOLOGY
2019, VOL. 53, NO. 9, 971–975
https://doi.org/10.1080/02786826.2019.1635677

AEROSOL RESEARCH LETTER

OPEN ACCESS Check for updates

Soot mass concentration sensor using quartz-enhanced photoacoustic spectroscopy

Philipp Breitegger[a], Mario A. Schriefl[a], Robert T. Nishida[b], Simone Hochgreb[b], and Alexander Bergmann[a]

[a]Institute of Electronic Sensor Systems, Graz University of Technology, Graz, Austria; [b]Department of Engineering, University of Cambridge, Cambridge, United Kingdom

ARTICLE HISTORY Received 21 January 2019; Accepted 9 June 2019

EDITOR Hans Moosmüller

1. Introduction

Photoacoustic spectroscopy (PAS) is a well-established method for sensitive and selective detection of trace gases such as NO_2 and CO_2 (Bozóki, Pogány, and Szabó 2011) as well as for the measurement of aerosol particles (e.g., Petzold and Niessner 1996). Commercial instruments for measuring soot concentrations of vehicle exhaust reach detection limits of 5 µg m^{-3} (corresponding to 50 Mm^{-1} for 1 s integration time) and offer a dynamic range of four orders of magnitude, enabling wide commercial success in the automotive industry (AVL List GmbH 2018; Giechaskiel et al. 2014; Lack et al. 2006). However, the high cost, size, and mass of conventional PAS systems (e.g., AVL Micro Soot Sensor [MSS]: $W \times H \times D =$ 483 mm × 400 mm × 555 mm, $m \approx 26$ kg) has limited its applicability for widespread use in ambient or environmental monitoring.

Photoacoustic instruments for soot measurement typically use an intensity modulated light source to transfer energy to soot particles (Petzold and Niessner 1996). Thermal relaxation of the soot particles produces an acoustic wave with a frequency that matches the modulation of the light source. For sufficiently small particles, the amplitude of the acoustic wave is directly proportional to the absorbed light energy and therefore to the soot mass absorption (Cremer et al. 2017). In conventional photoacoustic instruments the amplitude of the acoustic wave is usually amplified with a quality factor of around 10–80 (Bozóki, Pogány, and Szabó 2011; Rück, Bierl, and Matysik 2017; Yin et al. 2017) using organ-pipe-like acoustic resonators at resonance frequencies in the low kHz-range and detected with a conventional microphone (Bozóki, Pogány, and Szabó 2011; Schindler et al. 2004; Wolf et al. 2014; Yin et al. 2017). In contrast, quartz-enhanced photoacoustic spectroscopy (QEPAS) (Kosterev et al. 2002), may use mass-produced quartz tuning forks (QTF) with a resonant frequency f_0 of 32.768 kHz to detect acoustic waves with quality factor Q of around 8000 at ambient pressure. The two-orders of magnitude increase in quality factor over conventional PAS enables sensing of trace gases down to the ppb level (Patimisco et al. 2014). The signal in QEPAS is directly proportional to the ratio of Q to f_0. Thus, by designing a custom QTF with reduced f_0 and a similar Q, the signal strength can be further increased in QEPAS at similarly small sizes (Patimisco et al. 2017). Additional advantages are (a) a small and simple sensor design, as the QTF combines the resonator and electric transducer in one component and (b) high background noise immunity, due to the quadrupole characteristic of the QTF (Russell 2000). For a commercial QTF relative to conventional PAS, the effect of background noise is reduced by a factor of 46 (Rück, Bierl, and Matysik 2018).

While QEPAS has been used to study single, laser-trapped droplets (Cremer et al. 2016), this is the first proof of principle of measuring a continuous flow of

CONTACT Philipp Breitegger p.breitegger@tugraz.at Institute of Electronic Sensor Systems, Graz University of Technology, Graz 8010, Austria
Color versions of one or more of the figures in the article can be found online at www.tandfonline.com/uast.

soot aerosol. The off-the-shelf QTF is smaller than 5 mm in the longest dimension. Such piezoelectric QTFs are mass-produced for use as a clock in, e.g., quartz watches and are available for prices in the cent range. Therefore, in contrast to conventional PAS instruments, a QEPAS sensor enables significant miniaturization and cost reduction, which would enable large scale monitoring of sources with environmental impact (Breitegger and Bergmann 2016).

In this work, a measurement setup for a miniaturized soot sensor with QEPAS is reported. Specifically, measurements of mass concentrations of soot from a miniCAST soot generator are compared with those from an MSS, which is a common method to measure mass concentrations of soot.

2. Methods

The QEPAS sensor includes a QTF placed in an aluminum cell which allows optical access. The cell is of size 65 mm × 40 mm × 40 mm including all analog amplification circuits as well as temperature and pressure sensors. For proof of principle, the optical components were placed in line with the cell, increasing its length to 160 mm. It is expected that with little engineering effort, a miniaturization by at least a factor of two is feasible. A laser beam enters the cell through an N-BK7 window and is focused between the two prongs of the QTF approximately 0.7 mm from the top of the prongs for a strong signal (cf. Kosterev et al. 2002). The QTF is placed in a volume of only 1.6 cm^3. A photodiode, placed behind an optical filter, monitors the laser's power. A 30 mW optical power FLEXPOINT® Dot Laser Module (Laser Components GmbH) with 850 nm wavelength was chosen, as it has minimal spectroscopic cross-interference to any gases possibly contained in ambient or combustion related aerosol. Further, the module provides the advantages of relatively small size (length <57 mm), low cost (around 200 EUR), a moderate laser safety class, and an integrated laser driver enabling modulation. The laser is modulated by means of a function generator (National Instruments: Model PXI-5402) which shares the same synchronization clock as the acquisition module (National Instruments: Model PXI-6281). The laser is modulated at the resonance frequency of the QTF (Fox Electronics: NC38LF) f_0, determined by a frequency sweep as described below. The aerosol inlet and outlet to the cell are positioned perpendicular to the laser beam direction. Soot particles absorb the modulated laser light and transfer the energy to the surrounding gas molecules, which produces a sound wave of frequency f_0, which excites the QTF. The QTF produces a current from piezoelectric vibrations that is amplified with a transimpedance amplifier. The signal is acquired with the PXI-6281 card at 250 kilosamples per second and demodulated at f_0 with a lock-in amplifier with 1 s integration time, which is realized as a custom LabVIEW application on a personal computer. For further analysis, the QEPAS sensor is equipped with temperature, humidity, and absolute pressure sensors.

A miniaturized electronic solution containing a lock-in amplifier and microcontroller giving similar results is described by Kerschhofer, Breitegger, and Bergmann (2018). As compared to commercial available instruments (MSS by AVL, PAX by Droplet Measurement Technologies) this results in a reduction of size, mass and price by at least a factor of 50.

The experimental setup enables control of mass concentrations of soot particles as well as verification of the size distribution and number concentrations of soot using an MSS and a scanning mobility particle sizer (SMPS) as reference instruments. The setup is shown in Figure 1. The soot aerosol was generated

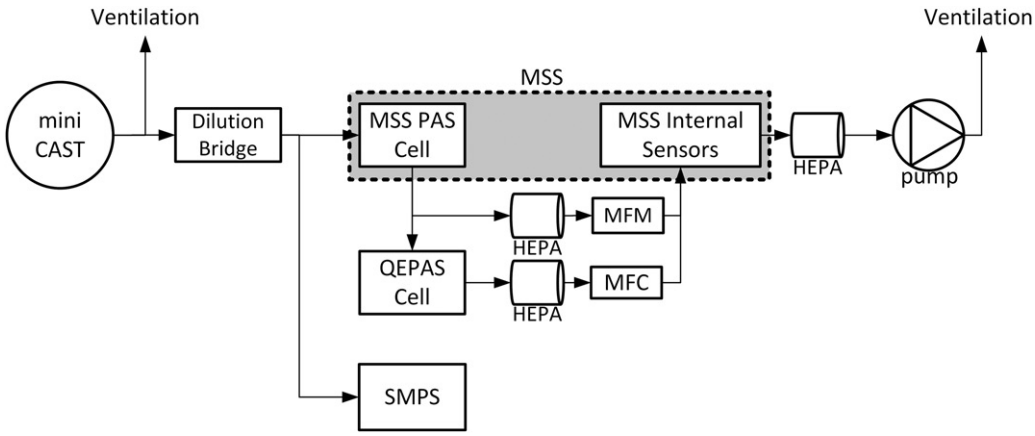

Figure 1. Setup to measure the linearity of the QEPAS cell.

with a miniCAST soot generator (Jing Ltd: Model 6204 Type B, flow settings: C_3H_8 (40 std cm^3 min^{-1}), oxidation air (500 std cm^3 min^{-1}), dilution air (5 std L min^{-1}), and quench gas N_2 (2 std L min^{-1}). The miniCAST was operated such that a size distribution with a geometric mean diameter of 78 nm was generated. To generate different soot concentrations a dilution bridge was used, which consists of a HEPA filter in parallel with a needle valve. The aerosol passed through the organ-like cell of a Micro Soot Sensor (AVL LIST GmbH) at a flow rate of 2 std L min^{-1}. To ensure the QEPAS cell measures the same particles as the MSS, the QEPAS cell was set in series to the PAS cell of the MSS. The flow rate through the QEPAS cell was fixed to 200 std cm^3 min^{-1} by means of a massflow controller (MFC; Vögtlin: Model GSC-B). The aerosol was also characterized using an SMPS (TSI Inc.: Model 3938).

For the determination of the soot mass concentration, the QEPAS signal was corrected for any changes in background. Before setting the dilution bridge to a new mass concentration, a HEPA filter was set in series with the mini CAST to obtain a background measurement. A sweep of the modulation frequency with 1 Hz resolution was performed around an interval of 10 Hz between the previously measured resonance frequency to obtain and adjust the modulation frequency accordingly. This was followed by the acquisition of the background signal for 30 s. The dilution was set such that the desired mass concentration was achieved, as measured by the MSS. The QEPAS signal was logged for 2 min. Each data point is made up of average of the last 30 s of the 2 min sampling time for both the QEPAS and MSS. Additionally, the size distribution of the produced soot was recorded with the SMPS for diagnostic reasons. To verify that the photoacoustic signal was immune to other effects, cross-interferences against NO_2, absolute pressure, and temperature variations were checked. Humidity remained almost constant during the measurements ((50 ± 3) % RH). The influence of humidity is the subject of further investigations. According to Arnott et al. (2003), operation of aerosol PA instruments below 65% RH is advised.

3. Results and discussion

Figure 2 shows the QEPAS signal as a function of the mass concentration of soot measured by the MSS. By performing a linear regression, the sensitivity was determined to be (8.08 ± 0.10) mV m^3 mg^{-1}. The coefficient of determination for the fit is $R^2 = 0.99$.

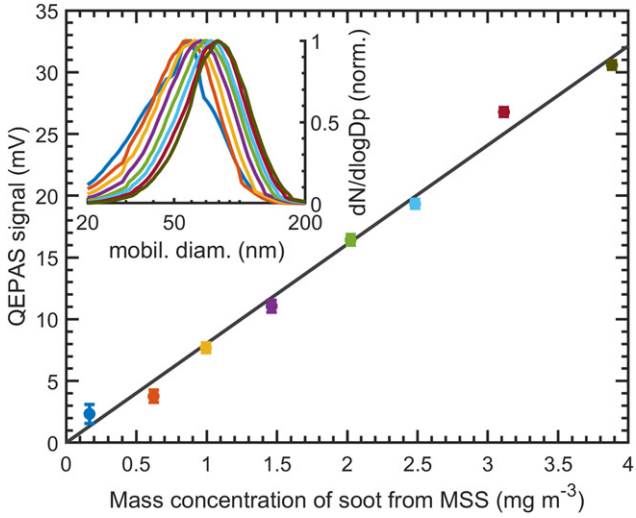

Figure 2. QEPAS signal in mV as a function of the mass concentration of soot particles measured by the micro-soot sensor (MSS). Error bars in the QEPAS signal represent the standard error relatively to the mean. Error bars for the mass concentrations as measured by the MSS are too small to be visible on this scale. The inset shows the measured size distributions with colors corresponding to each point. The best fit line assumes identical zero offsets at zero.

Each datapoint has a different color, which corresponds to the mobility size distribution shown in the inset of Figure 2. Throughout the measurements, the geometric mean diameter increased from 49 nm for the lowest concentration to 78 nm when the dilution bridge was at the lowest dilution and fully open. Deviations of the measurements from a linear slope in Figure 2 for larger particle diameters could not be seen within the investigated size ranges (Cremer et al. 2017).

Important considerations for aerosol sensors are long-term stability as well as the decrease in uncertainty due to increased time for signal averaging. This is commonly analyzed by the Allan deviation methodology (Werle, Mücke, and Slemr 1993), which consists in the standard deviation as a function of averaging time. Figure 3 shows the Allan deviation for a continuous sample drawn from HEPA filtered room air at 200 std cm^3 min^{-1}. The Allan deviation decreases up to an averaging time of 19 s. After that time, drift occurs, therefore, the 3σ noise equivalent concentration for 19 s would correspond to 80 µg m^{-3}. In this publication, a 30 mW laser module was selected to demonstrate the applicability of QEPAS for aerosol measurements. For easier compliance with laser regulations, the proof of principle experiments were performed with a low power laser module. Nevertheless by increasing the laser power to, e.g., 500 mW, we expect the limit of detection to be lowered to

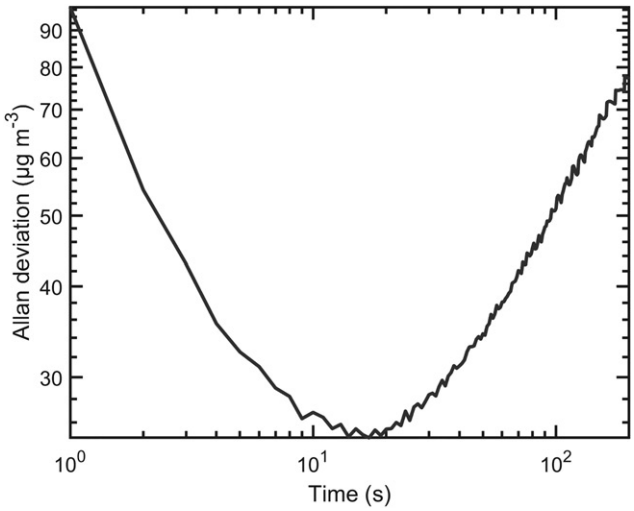

Figure 3. Allan deviation of the QEPAS sensor as a function of averaging time when using suction by a nozzle of ambient, filtered air.

4.8 µg m^{-3} without increasing the over-all sensor size. Furthermore, preliminary tests indicate that sensor fouling due to soot accumulation on the QTF was not detectable at an average soot loading of 2 mg/m^3 for 8 h.

4. Conclusions

In this work, soot mass concentration measurements using QEPAS are reported for the first time. A custom made QEPAS cell with designated aerosol sampling ports operated with a 30 mW laser module resulted in a limit of detection of 80 µg m^{-3} with an averaging time of 19 s. Given the small size, weight, and cost the instrument is suitable for environmental measurements close to the emission source. One possible application could be monitoring failures of particulate filters for diesel or gasoline engines (e.g., periodical technical inspections as well as real driving emission measurements). The results show excellent linearity with the reference instrument (MSS) over a wide range of mass concentrations of soot with negligible sensor fouling due to heavy soot loading.

Acknowledgments

The authors acknowledge AVL List GmbH for loaning the Micro Soot Sensor for the experiment.

Funding

Open access publication is supported by the TU Graz Open Access Publishing Fund.

ORCID

Philipp Breitegger http://orcid.org/0000-0003-3049-4921
Robert T. Nishida http://orcid.org/0000-0002-9820-1569
Simone Hochgreb http://orcid.org/0000-0001-7192-4786
Alexander Bergmann http://orcid.org/0000-0003-3343-8319

References

Arnott, W. P., H. Moosmüller, P. J. Sheridan, J. A. Ogren, R. Raspet, W. V. Slaton, J. L. Hand, S. M. Kreidenweis, and J. L. Collett. Jr. 2003. Photoacoustic and filter-based ambient aerosol light absorption measurements: Instrument comparisons and the role of relative humidity. *J. Geophys. Res.* 108 (D1):4034–4044. doi:10.1029/2002JD002165.

AVL List GmbH. 2018. Avl Micro Soot Sensor Operating Manual, Rev. 14. Graz, Austria.

Bozóki, Z., Pogány, A., and Szabó, G. 2011. Photoacoustic instruments for practical applications: Present, potentials, and future challenges. *Appl. Spectrosc. Rev.* 46 (1):1–37.

Breitegger, P., and A. Bergmann. 2016. Air quality and health effects – How can wireless sensor networks contribute? A critical review. In *2016 International Conference on Broadband Communications for Next Generation Networks and Multimedia Applications (CoBCom)*, vol. 9, 1–8. Graz, Austria: IEEE. http://ieeexplore.ieee.org/document/7593507/.

Cremer, J. W., K. M. Thaler, C. Haisch, and R. Signorell. 2016. Photoacoustics of single laser-trapped nanodroplets for the direct observation of nanofocusing in aerosol photokinetics. *Nat. Commun.* 7 (1):1–7. doi:10.1038/ncomms10941.

Cremer, J. W., P. A. Covert, E. A. Parmentier, and R. Signorell. 2017. Direct measurement of photoacoustic signal sensitivity to aerosol particle size. *J. Phys. Chem. Lett.* 8 (14):3398–3403. doi:10.1021/acs.jpclett.7b01288.

Giechaskiel, B., M. Maricq, L. Ntziachristos, C. Dardiotis, X. Wang, H. Axmann, A. Bergmann, and W. Schindler. 2014. Review of motor vehicle particulate emissions sampling and measurement: From smoke and filter mass to particle number. *J. Aerosol Sci.* 67:48–86. doi:10.1016/j.jaerosci.2013.09.003.

Kerschhofer, A., P. Breitegger, and A. Bergmann. 2018. Laser driver and analysis circuitry development for Quartz-Enhanced photoacoustic spectroscopy of NO2 for IoT purpose. *Proceedings.* 2 (13):1062. doi:10.3390/proceedings2131062.

Kosterev, A. A., Y. A. Bakhirkin, R. F. Curl, and F. K. Tittel. 2002. Quartz-enhanced photoacoustic spectroscopy. *Opt. Lett.* 27 (21):1902.

Lack, D. A., E. R. Lovejoy, T. Baynard, A. Pettersson, and A. R. Ravis- Hankara. 2006. Aerosol absorption measurement using photoacoustic spectroscopy: Sensitivity, calibration, and uncertainty developments. *Aerosol Sci. Technol.* 40 (9):697–708. doi:10.1080/02786820600803917.

Patimisco, P., A. Sampaolo, H. Zheng, L. Dong, F. K. Tittel, and V. Spagnolo. 2017. Quartz-enhanced photoacoustic spectrophones exploiting custom tuning forks: A review. *Adv. Phys.* 2 (1):169–187. doi:10.1080/23746149.2016.1271285.

Patimisco, P., G. Scamarcio, F. Tittel, and V. Spagnolo. 2014. Quartz-enhanced photoacoustic spectroscopy: A review. *Sensors*. 14 (4):6165–6206. doi:10.3390/s140406165.

Petzold, A., and R. Niessner. 1996. Photoacoustic soot sensor for in-situ black carbon monitoring. *Appl. Phys. B.* 63 (2):191–197. doi:10.1007/BF01095272.

Rück, T., R. Bierl, and F. M. Matysik. 2017. Low-cost photoacoustic NO_2 trace gas monitoring at the pptV-level. *Sens. Actuat. A.* 263 (2):501–509. doi:10.1016/j.sna.2017.06.036.

Rück, T., R. Bierl, and F. Michael Matysik. 2018. NO_2 trace gas monitoring in air using off-beam quartz enhanced photoacoustic spectroscopy (QEPAS) and interference studies towards CO_2, H_2O and acoustic noise. *Sens. Actuat. B.* 255 (2):2462–2471. doi:10.1016/j.snb.2017.09.039.

Russell, D. A. 2000. On the sound field radiated by a tuning fork. *Am. J. Phys.* 68 (12):1139–1145. doi:10.1119/1.1286661.

Schindler, W., C. Haisch, H. A. Beck, R. Niessner, E. Jaco, and D. Rothe. 2004. A photoacoustic sensor system for time resolved quantification of diesel soot emissions. In *SAE 2004 World Congress & Exhibition*, SAE International in United States, March 8. http://papers.sae.org/2004-01-0968/. https://www.sae.org/content/2004-01-0968/.

Werle, P., R. Mücke, and F. Slemr. 1993. The limits of signal averaging in atmospheric trace-gas monitoring by tunable diode-laser absorption spectroscopy (TDLAS). *Appl. Phys. B.* 57 (2):131–139.

Wolf, J. C., A. Danner, R. Niessner, and C. Haisch. 2014. NO_2 measurement artifacts in the presence of soot. *Anal. Bioanal. Chem.* 406 (2):447–453. doi:10.1007/s00216-013-7495-8.

Yin, X., L. Dong, H. Wu, H. Zheng, W. Ma, L. Zhang, W. Yin, S. Jia, and F. K. Tittel. 2017. Sub-ppb nitrogen dioxide detection with a large linear dynamic range by use of a differential photoacoustic cell and a 3.5 W blue multimode diode laser. *Sens. Actuat. B.* 247:329–335. doi:10.1016/j.snb.2017.03.058.